Laser and Particle Beams (2004), *22*, 175–181. Printed in the USA.

DOI: 10.1017/S0263034604222133

Ion acceleration in overdense plasma by short laser pulse

O. SHOROKHOV AND A. PUKHOV
Institut für Theoretische Physik I, Heinrich-Heine-Universität Düsseldorf, Germany
(RECEIVED 21 May 2003; ACCEPTED 31 August 2003)

Abstract

We consider ion acceleration at the front surface of overdense plasma by a short laser pulse. In this configuration, the laser ponderomotive pressure pushes the background electrons, and a double layer is produced at the boundary of the overdense region. The ions are accelerated by the electrostatic field of the double layer. If the laser intensity is so large that the plasma becomes relativistically transparent, then ion trapping in the running double layer and acceleration to relativistic energies is possible. We study this physics using one-dimensional particle-in-cell simulations. Ion acceleration in one- and two-component plasmas is considered. It is shown that the proton acceleration is more effective when they represent only a small dope to the heavy background ions.

Keywords: Ion acceleration; Laser–plasma interaction; Relativistic effects

1. INTRODUCTION

Acceleration of charged particles to high energies is one of the most interesting applications of intense short laser pulses. A number of recent experiments (Clark *et al.*, 2000; Krushelnick *et al.*, 2000; Maksimchuk *et al.*, 2000; Roth *et al.*, 2000, 2002; Snavely *et al.*, 2000; Santala *et al.*, 2001; Borghesi *et al.*, 2002; Zepf *et al.*, 2003) and even heavier ions (Hegelich *et al.*, 2002) have demonstrated that protons can be efficiently accelerated in laser–plasma experiments. Different acceleration mechanisms have been proposed for explanation of the experimental results. In the underdense plasma channels (Pukhov & Meyer-ter-Vehn, 1996; Krushelnick *et al.*, 2000) this is the Coulomb explosion of the electron-cavitated region near the laser channel axis. In the experiments of overdense foils, two major explanations exist (Pukhov, 2001; Wilks *et al.*, 2001). First, there is a direct ponderomotive push at the front surface. This leads to a double-layer formation and ion acceleration. Second, there is the so-called target normal sheath acceleration (TNSA). The TNSA suggests that the laser pulse produces hot electrons at the front surface. Then, they propagated through the foil and generate a space charge sheath at the rear surface of the target. The electrostatic field of this space charge pulls the ions sitting on the rear surface and accelerates them to high energies. In most of these experiments, very powerful lasers have been used with the pulse energy in the range 100–1000 J and powers of 100–1000 TW.

Address correspondence and reprint requests to: O. Shorokhov, Institut für Theoretische Physik I, Heinrich-Heine-Universität Düsseldorf, D-40225, Germany. E-mail: oleg@thphy.uni-duesseldorf.de

In this article we are studying in detail ion acceleration at the front surface of the plasma layer. Our aim is to understand what is the scaling of the maximum attainable ion energy as a function of the laser intensity. Particularly, we are interested in the possibility of proton acceleration to some 300–600 MeV energy using the lowest possible laser pulse energy. Protons in this particular energy range might be used, for example, for cancer therapy in medicine (Kraft, 2001; Esirkepov *et al.*, 2002). To achieve these energies with the TNSA mechanism would require not only very high laser intensities to heat electrons to the comparable energies, but also pretty long pulse durations, because the electric fields in the Debye sheath represent only a small fraction of the laser ones. In this sense, short and intense lasers applied to the front surface can be more suitable for ion acceleration with high repetition rate.

The direct coupling of the laser energy to the protons begins at very high laser intensities above the proton relativistic threshold $I > I_p = (m_i/m_e)^2 I_0 \sim 10^{24}$ Wμm^{2}cm^{-2}. Here I_0 is the electron relativistic threshold, $I_0 \lambda^2 = 1.37 \times 10^{18}$ Wμm^{2}cm^{-2}, where λ is the laser wavelength. In this article we study intensities still well below I_p. Yet, we show that the laser-induced plasma fields may be sufficient to accomplish the proton acceleration to nearly relativistic energies.

2. ION ACCELERATION AT THE FRONT SURFACE

The energy of accelerated ions can be easily estimated if the plasma contains just one ion species and is overdense for the

laser pulse (Wilks *et al.*, 1992). Then one can use the momentum conservation law. The laser light pressure can be considered as a momentum flux

$$P_l = \frac{I}{c} = n_{cr} mc^2 \frac{a^2}{2}, \tag{1}$$

where $a = eA/mc^2$ is the dimensionless amplitude of the laser vector potential, and $n_{cr} = m\omega^2/4\pi e^2$ is the critical density. The momentum flux transported by the ions is

$$P_i = n_i \frac{p_i^2}{M_i \gamma_i}, \tag{2}$$

where n_i is the ion density, M_i is the ion mass, p_i is the mean ion momentum, and $\gamma_i = \sqrt{1 + (p_i/M_i c)^2}$ is the relativistic γ factor.

If the laser pulse is completely absorbed, then we must set $P_i = P_l$. If, however, the laser pulse is back reflected, then $P_i = 2P_l$. In the general case of the absorption rate $0 \leq \eta \leq 1$ we have

$$P_i = (2 - \eta) P_l. \tag{3}$$

This gives the ion energy estimation

$$E_i = \frac{p_i^2}{(1 + \gamma_i) M_i} = (2 - \eta) \frac{n_{cr}}{n_i} \frac{a^2}{2} mc^2. \tag{4}$$

The plasma layer remains overdense for a relativistically intense laser pulse only if $n_e/n_{cr} > a/2$, where $n_e = Zn_i$ is the electron density and Z is the ion charge. At higher intensities, the plasma is relativistically transparent. Setting the laser amplitude at the boundary of relativistic transparency, $a \approx 2Zn_i/n_{cr}$, we estimate the maximum ion energy as

$$E_i^{max} \approx (2 - \eta) Z \frac{a}{m} c^2. \tag{5}$$

The estimations (4) and (5) are based on the fundamental law of momentum conservation. They are insensitive to the particular interaction physics. The only assumption made here is that all the plasma ions are equivalent, that is, a single species plasma is given.

However, the experiments show that whatever material is irradiated by the laser, it is usually protons that get accelerated first. If plasma is a mixture of different species, then a small portion of ions with a large charge-to-mass ratio can be accelerated to higher energies than is allowed by the simple limits (4) and (5). In this case, the particular mechanism of acceleration is very important.

We consider here the so-called "ion wakefield acceleration" mechanism. It works when some energetic ions get trapped into an electrostatic plasma wave. Let us assume that the plasma wave is running with the phase velocity v_p, that is, all the density perturbations and the potential are functions of $\xi = x - v_p t$. If the background ions oscillating in the field of this wave get velocities comparable with the wave phase velocity, $v_i \sim v_p$, then they are trapped and may be accelerated further to very high energies. This mechanism is analogous to the well-known electron trapping in plasma waves (Esarey & Pilloff, 1995). Below we estimate the laser intensity and plasma parameters needed for such ion trapping.

3. MODEL FOR ION TRAPPING IN A RUNNING PLASMA WAVE

We assume that the plasma slab has initially a uniform density distribution

$$n(x) = \begin{cases} 0, & \text{for} \quad x < 0 \\ n, & \text{for} \quad x \geq 0. \end{cases} \tag{6}$$

We also assume that the ponderomotive pressure of the laser pulse works as a "snowplow" and sweeps the background electrons forward until a buildup of the electrostatic field equilibrates the pressure. In the laboratory system of reference (K), the snowplow moves with the plasma wave phase velocity v_p.

When we transform to the reference system co-moving with the plasma wave (K') we have noncompensated charge density *ne* behind the shock wave. For the electrostatic field and the electrostatic potential (in K') we obtain the relations

$$\frac{dE_x'}{dx'} = \begin{cases} 4\pi n' e, & \text{for} \quad 0 \leq x' \leq d \\ 0, & \text{for} \quad x' > d, \end{cases} \tag{7}$$

where

$$d = \frac{E_{max}'}{4\pi n' e}. \tag{8}$$

Because of the plasma quasineutrality, the wave of compression is followed by a wave of rarefaction and a quasisymmetric picture of electric field and potential is formed:

$$E_x'(x) = \begin{cases} 4\pi n' e x', & \text{for} \quad |x'| \leq d \\ 0, & \text{for} \quad |x'| > d, \end{cases} \tag{9}$$

$$\phi'(x') = -\int_0^{x'} E_x'(\xi)\, d\xi = \begin{cases} -2\pi n' e x'^2, & \text{for} \quad |x'| \leq d \\ -\dfrac{E_{max}'^2}{8\pi n' e}, & \text{for} \quad |x'| > d. \end{cases} \tag{10}$$

We choose the integration constant to have $\phi'(0) = 0$. In the reference system K', the charge density and the electric field form a stationary periodic structure with the period $2d$. This structure moves behind the laser pulse with the phase velocity v_p. A typical structure of such a wave obtained from a one-dimensional PIC simulation is shown in Figure 1.

https://doi.org/10.1017/S0263034604222133 Published online by Cambridge University Press

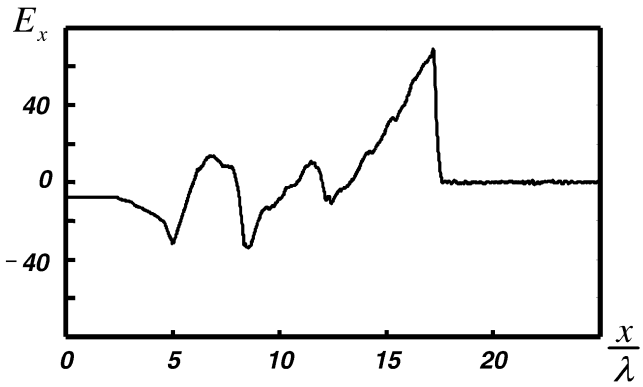

Fig. 1. Plasma wave obtained in the PIC simulation. The laser amplitude $a = 60$, the plasma density $n = 10n_{cr}$. The maximum electric field is close to the laser amplitude.

The electric field E_{max} can be found from the condition of equilibrium with the laser ponderomotive pressure at the front of the wave. Doing this, we obtain the estimation $E_x \approx E_0$, where E_0 is the amplitude of the laser pulse electric field.

Making a transition from K to K' and taking into account that Lorenz transformation does not change longitudinal components of fields, we obtain

$$E'_{max} = E'_x(x' = d) \approx E_0, \tag{11}$$

where

$$x' = \frac{x - v_p t}{\sqrt{1 - \frac{v_p^2}{c^2}}}. \tag{12}$$

Integrating, we obtain the potential difference over the half plasma wavelength $\Delta\Phi = \phi(d) - \phi(0)$:

$$e|\Delta\Phi'| = m_e c^2 \left(\frac{n_{cr}}{n'}\right)\frac{a_0^2}{2}. \tag{13}$$

Here a_0 is the usual dimensionless laser amplitude

$$a_0 = \frac{eA}{m_e c^2}, \quad E_0 = \frac{m_e \omega_0 c}{e}\, a_0. \tag{14}$$

Because the plasma wave is driven by the laser pulse, we can postulate with good accuracy that the wave phase velocity is equal to the laser group velocity, if the plasma is relativistically transparent:

$$v_p = v_{gr}^{las} \approx \sqrt{1 - \frac{\omega_p^2}{\omega_0^2 \langle\gamma\rangle}}, \tag{15}$$

where v_{gr}^{las} is the laser pulse group velocity and $\langle\gamma\rangle$ is an averaged relativistic γ factor of plasma electrons.

When an ultrarelativistically intense laser pulse propagates in plasma, we can use the estimation

$$\langle\gamma\rangle \sim \frac{a_0}{2} \tag{16}$$

and obtain

$$\frac{v_p}{c} \approx \sqrt{1 - \frac{n}{n_{cr}}\frac{2}{a_0}}, \tag{17}$$

$$\gamma_p = \frac{1}{\sqrt{1 - \frac{v_p^2}{c^2}}} = \sqrt{\frac{n_{cr}}{n}\frac{a_0}{2}}, \quad a_0 \geq \frac{2n}{n_{cr}}. \tag{18}$$

To describe the ion motion in the laser-generated wave, we introduce the Hamilton function $H(x, p, t)$. In the moving system of reference K', the plasma wave can be considered as quasistationary and the Hamiltonian has the form $H'(x', p') = E'_i + e\phi'(x')$. The energy conservation along an ion trajectory provides the equation for the trajectories $H'(x', p') = E' = const$.

Now we use Eq. (12) and express the ion energy through the momentum p_i in the laboratory frame. We obtain

$$H'(x, p_i) = \frac{\sqrt{p_i^2 c^2 + m_i^2 c^4} - v_p p_i}{\sqrt{1 - \frac{v_p^2}{c^2}}} + e\phi'\left(\frac{x - v_p t}{\sqrt{1 - \frac{v_p^2}{c^2}}}\right). \tag{19}$$

At this point, we introduce new dimensionless variables

$$\frac{v}{c} \to v, \qquad \frac{p_i}{m_i c} \to p_i, \qquad \frac{n}{n_{cr}} \to n, \qquad y = \frac{x - v_p t}{d\sqrt{1 - v_p^2}} \tag{20}$$

and obtain

$$h'(x, p_i) = \frac{H'}{m_i c^2} = \frac{\sqrt{1 + p_i^2} - v_p p_i}{\sqrt{1 - v_p^2}} + \frac{e}{m_i c^2}\,\phi'\left(\frac{x - v_p t}{\sqrt{1 - v_p^2}}\right). \tag{21}$$

We substitute now the particular form of the potential (10), take into account that the electron density $n = n'/\sqrt{1 - v_p^2}$, and obtain

$$h'(y, p_i) = \frac{\sqrt{1 + p_i^2} - v_p p_i}{\sqrt{1 - v_p^2}} - \frac{m_e}{m_i}\frac{1}{n\sqrt{1 - v_p^2}}\frac{a^2}{2} y^2. \tag{22}$$

The equation $h'(y, p_i) = 1$ gives us the separatrix. It separates the trapped ions with $h' < 1$ from the passing ions with $h' > 1$. The ion trajectories and the separatrix for different laser amplitudes are shown in Figure 2.

When the separatrix touches the axis $p = 0$, then even ions initially at rest can be trapped in the wave. This condition can be written as

https://doi.org/10.1017/S0263034604222133 Published online by Cambridge University Press

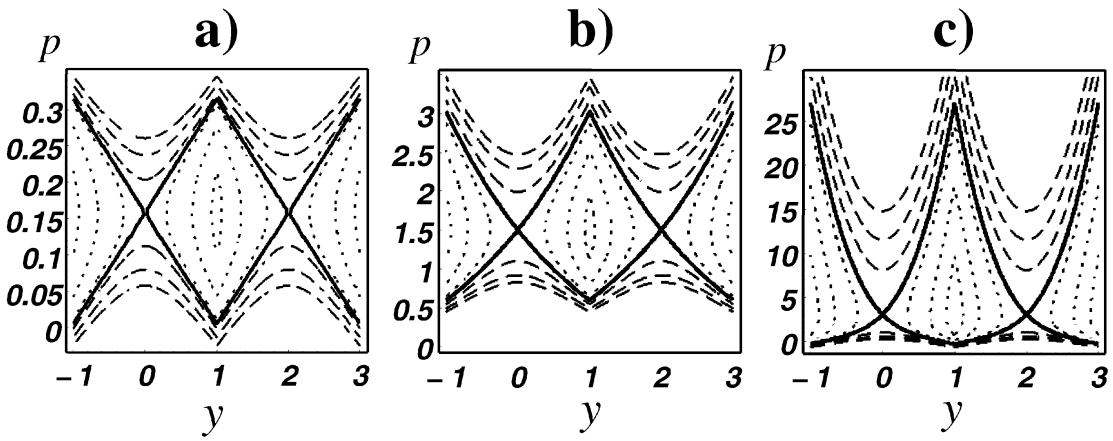

Fig. 2. Trajectories of protons in the (y, p) phase space. The plasma density is assumed to be $n = 10n_{cr}$. The laser amplitude is $a = 20.5$ (a), $a = 65$ (b), $a = 200$ (c).

$$1 - \frac{m_e}{m_i}\frac{a_{tr}^2}{2n} = \frac{1}{\gamma_p}. \tag{23}$$

There are two distinct regions of parameters when the ions can be trapped into the plasma wave. The first one corresponds to low laser group velocities, when the laser is just at the verge of the relativistic transparency: $a \geq 2n$, $\gamma_p \approx 1$. In this case, the plasma wave is very slow and it is easy to fulfill the ion trapping condition $v_i \approx v_p$. The phase portrait in Figure 2a corresponds to this case. When the laser amplitude increases, the lower bound of the separatrix rises and the ions at rest cannot be trapped anymore Figure 2b. Another region of parameters, where the separatrix goes down to the axis $p = 0$ corresponds to $\gamma_p \gg 1$. Here we have a very simple estimation for the threshold laser amplitude:

$$a_{tr} \approx \sqrt{2\frac{m_i}{m_e}n}. \tag{24}$$

This case is shown in Figure 2c.

This splitting can be interpreted in the following way. If one considers ion trapping in a moving potential well, then two factors have influence on the trapping process. First, how deep the well is (how large the potential difference is) and second, how quickly the well moves. In the case of Figure 2a, the potential difference is relatively small, but the well moves very slowly with respect to the ions. The interaction lasts for a long time and the ions are able to gain enough energy to be trapped. When the well starts to move faster, it races through the ions too quickly, and ions can be trapped only at relatively large amplitudes of the well (Fig. 2b,c).

The laser intensity corresponding to the threshold amplitude (24) can be 1 to 2 orders of magnitude lower than the proton relativistic intensity I_p, yet, pretty large. On the other hand, laser pulses that allow for the relativistic transparency of overdense plasmas can become available in the nearest future. We have seen (Fig. 2a) that already at the relativistic transparency threshold the protons can be trapped in the plasma wave.

4. NUMERICAL SIMULATIONS

To investigate the ion acceleration near the front surface and the propagation through the plasma we use one-dimensional particle-in-cell simulations. The laser pulse is emitted at the left side of the simulation domain. It first propagates through a vacuum region and then interacts with a slab of overdense plasma. The plasma slab has constant density n with a sharp boundary. For the simulations we use the one-dimensional version of the code Virtual Laser Plasma Laboratory (Pukhov & Meyer-ter-Vehn, 1997, 1998; Pukhov, 1999).

The simulation box is 50λ long, where $\lambda = 2\pi(c/\omega_0)$ is the laser wavelength. We use absorbing boundary conditions: particles that achieve the boundaries are removed from the simulation box, fields are absorbed completely on the boundaries. The laser pulse has a cosine intensity profile: $a = a_0 \cos(\pi t/\tau)\cos(\omega_0 t)$ with $\omega_0 \tau = 2\pi \cdot 10$. The laser is circularly polarized.

We perform a parametric study of the ion acceleration by varying the laser pulse amplitude a_0 in the range from $a = 1$ to $a = 100$ and the plasma density n from $5n_{cr}$ to $10n_{cr}$.

In general, we consider plasma consisting of three types of particles: electrons, heavy ions, and protons. We model heavy ion presence using either infinitely heavy "nailed" ions or ions with deuteron charge-to-mass ratio. Thus, we have for the ion concentration

$$n_i = n_p + n_h, \tag{25}$$

where n_p is the proton concentration, and n_h is the heavy ion concentration.

Figure 3 shows the maximum proton energy obtained in our simulation for laser–plasma interaction with pure hydrogen (the solid curve), with 10% hydrogen–90% deuterium

https://doi.org/10.1017/S0263034604222133 Published online by Cambridge University Press

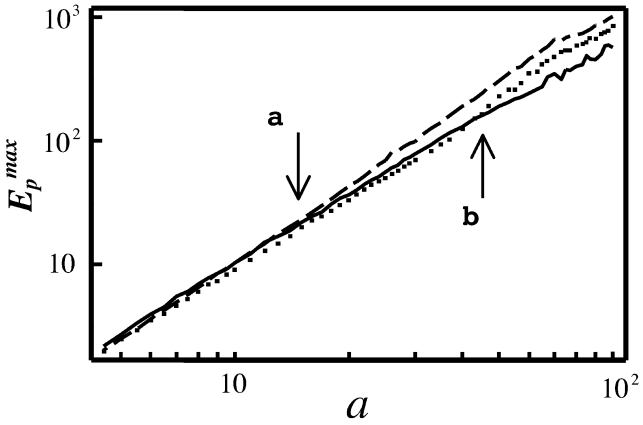

Fig. 3. The maximum proton energy observed in the simulation as a function of the laser pulse amplitude in double-logarithmic scales. The pulse length $\tau = 10\lambda$. The electron density $n = 10n_{cr}$. The simulation is done for the cases of pure hydrogen (the solid curve), 10% hydrogen–90% deuterium mixture (the dotted line), and 10% hydrogen–90% heavy "nailed" ions mixture (the broken line).

mixture (the dotted line), and 10% hydrogen–90% heavy nailed ions mixture (the broken line).

One sees from Figure 3 that the maximum proton energy scales quadratically with the laser amplitude, $E_p^{max} \sim a^2$ for all types of considered plasmas at moderate intensities. For the pure hydrogen plasma the energy keeps the same dependence in the full scanned range of laser amplitudes. In the case of mixed plasmas, however, we observe a change in the scaling after some critical amplitude is reached. This is seen as branching points in Figure 3 (pointed by arrows). The first branching point (a) is observed for the mixture of a small amount of protons in a background of nailed ions. This first break in the scaling approximately corresponds to amplitude, when plasma becomes relativistically transparent. This results in a generation of the plasma wave, which traps the lightest ions, protons, and accelerates them. Of course, the plasma wave can be generated in a purely hydrogenic plasma as well. In this case, however, it is destroyed very fast, because all the plasma ions get trapped simultaneously. In addition, the ponderomotive scaling (5) obtained from the momentum conservation must be valid for the single-species plasma. The scaling break in the proton–deuteron mixture happens at much larger laser amplitudes (point b) than for the proton–immobile ions mixture. The reason is that the charge-to-mass ratio between the protons and deuterons is not very large and at low laser amplitudes, the deuterons also start to move and disturb significantly the plasma wave structure.

Figure 4 presents more detailes of the laser pulse interaction with plasma. The two types of the interaction can be clearly distinguished in this picture: the "light pressure regime" (column I) and the "wake field regime" (column II). Panel b in column I shows that the electrostatic plasma field does not change its sign. It corresponds to the double layer produced at the plasma boundary by the ponderomotive pressure of the laser. Panel b in column II clearly corresponds to a decaying plasma wave. The wave decay is due to the particle acceleration in the wave. In the second case, the plasma became relativistically transparent for the laser pulse.

Using the estimation for the plasma refraction index

$$n_R = \sqrt{1 - \frac{n_e}{n_{cr}\langle\gamma\rangle}} \tag{26}$$

and taking into account (16) we find that for this particular density, $n = 10n_{cr}$, the plasma becomes transparent for $a_0 \geq 20$. The plasma wave generation and the form of the proton longitudinal phase space (panels a in Fig. 4), make the proton acceleration mechanism evident.

We mention that the trapping condition (24) for protons at rest is not fulfilled. Yet, the protons get trapped. This can be explained by the fact that when the head of the laser pulse reaches the plasma boundary, the plasma is changing from the overdense reflection to relativistic transparency. As it is seen from Figure 2a, the protons can be trapped and preaccelerated in this regime. Later, when the laser intensity continues to grow, these preaccelerated protons get trapped into the plasma wave and the acceleration continues.

5. DISCUSSION

We have studied proton acceleration to nearly relativistic energies by intense laser pulses at the front of an overdense plasma slab. A large number of protons with up to gigaelectron volt energies can be produced by laser pulses with reasonable intensities. We have shown that if the plasma is a mixture of a small number of protons and a large number of heavier ions, then the proton acceleration is more efficient.

In the case of a single-species plasma, the maximum ion energy scales according to the simple ponderomotive formula (5). Yet, when the plasma consists of a mixture of light and heavy ions, the lighter ions are preferentially accelerated. At the verge of the plasma relativistic transparency, the simple ponderomotive scaling breaks, and the ion trapping in the laser wakefield begins. In our PIC simulations, we observe that the proton energies in this case can be 3–4 times larger than the ponderomotive limit (5).

The simulation example presented in Figure 4 was done for the laser amplitude $a = 50$. This corresponds to the laser intensity $I \approx 7 \times 10^{21}$ W/cm^2 for a 1-μm laser wavelength. One may expect that such laser pulses will be available in the nearest future. We have observed proton energies of up to 300 MeV for this laser pulse parameters.

We should note that the goal of this article is to investigate the longitudinal ion acceleration over a wide range of parameters using a number of numerical experiments. Yet, the considered one-dimensional model abstracts from quite important multidimensional effects such as the hole boring and laser self-focusing/filamentation (Pukhov & Meyer-ter-Vehn, 1997, 1998; Sentoku *et al.*, 2000), "Coulomb explo-

https://doi.org/10.1017/S0263034604222133 Published online by Cambridge University Press

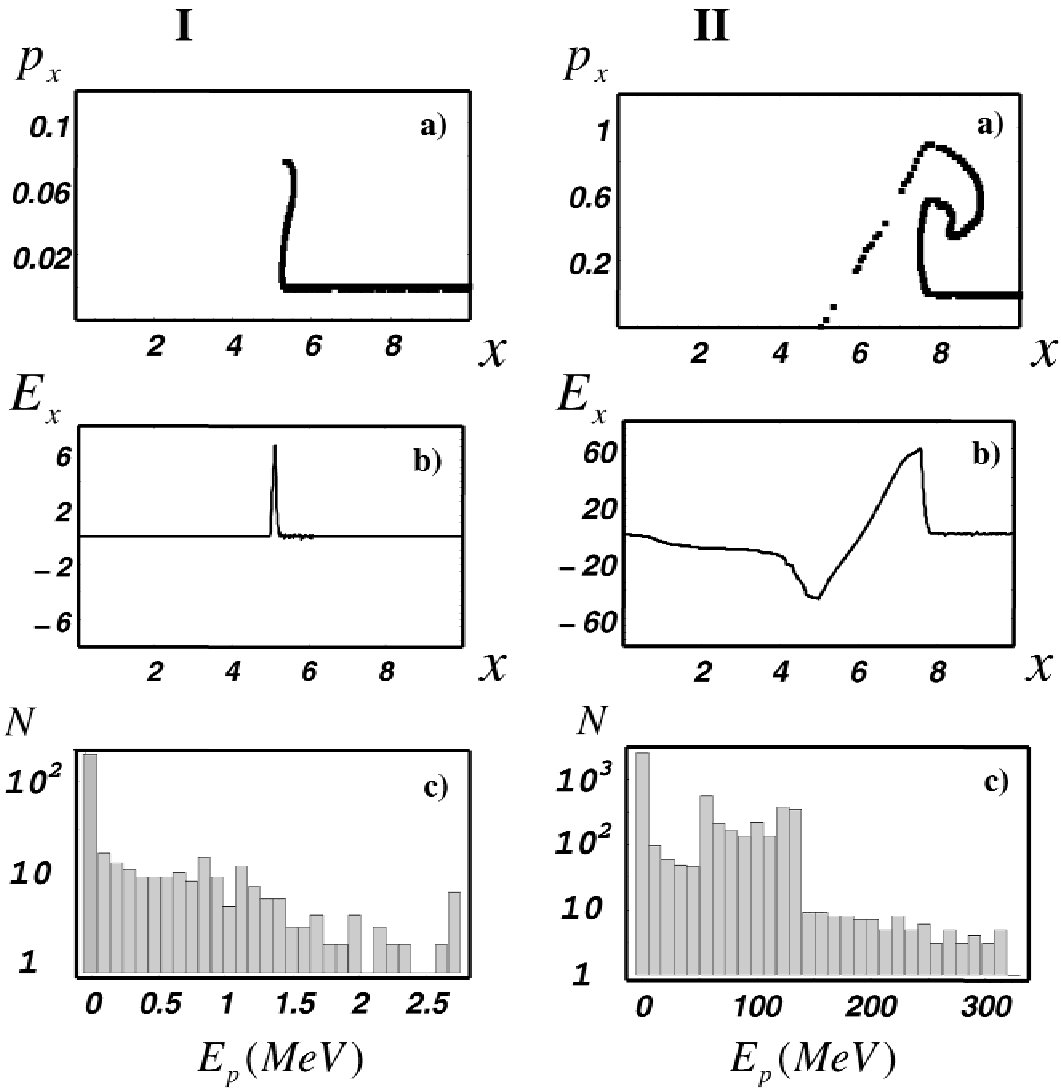

Fig. 4. Results of the PIC simulation. The laser pulse is 10λ long. The plasma electron density $n = 10n_{cr}$. The plasma consists of a mixture of protons and heavy "nailed" ions, $n_h/n_p = 9$. Columns I and II correspond to the laser pulse amplitudes $a = 5$ and $a = 50$, respectively. The snapshots are taken when the pulse maximum reaches the plasma boundary. a: the phase space of the protons (x, p_x). b: the longitudinal electric field. c: the proton energy spectra.

sion" and inductive electric field generation (Esirkepov *et al.*, 1999), and so forth. The question of how these effects modify the mechanism described in this article will be clarified later in the full three-dimensional PIC simulations.

ACKNOWLEDGMENTS

This work was supported in part by DFG, Humbold foundation, and BMBF/Bonn.

REFERENCES

Borghesi, M., Campbell, D.H., Schiavi, A., Haines, M.G., Willi, O., MacKinnon, A.J., Patel, P., Gizzi, L.A., Galimberti, M., Clarke, R.J., Pegoraro, F., Ruhl, H. & Bulanov, S. (2002). Electric field detection in laser-plasma interaction experiments via the proton imaging technique. *Phys. Plasmas* **9**, 2214–2220.

Clark, E.L., Krushelnick, K., Davies, J.R., Zepf, M., Tatarakis, M., Beg, F.N., Machacek, A., Norreys, P.A., Santala, M.I.K., Watts, I. & Dangor, A.E. (2000). Measurements of energetic proton transport through magnetized plasma from intense laser interactions with solids. *Phys. Rev. Lett* **84**, 670–673.

Esarey, E. & Pilloff, M. (1995). Trapping and acceleration in nonlinear plasma waves. *Phys. Plasmas* **2**, 1432–1436.

Esirkepov, T.Zh., Bulanov, S.V., Nishihara, K., Tajima, T., Pegoraro, F., Khoroshkov, V.S., Mima, K., Daido, H., Kato, Y., Kitagawa, Y., Nagai, K. & Sakabe, S. (2002). Proposed double-layer target for the generation of high-quality laser-accelerated ion beams. *Phys. Rev. Lett* **89**, 175003.

Esirkepov, T.Zh., Sentoku, Y., Mima, K., Nishihara, K., Califano, F., Pegoraro, F., Naumova, N.M., Bulanov, S.V., Ueshima, Y., Liseikina, T.V., Vshivkov, V.A. & Kato,

https://doi.org/10.1017/S0263034604222133 Published online by Cambridge University Press

Y. (1999). Ion acceleration by superintense laser pulses in plasmas. *JETP Lett* **70**, 82–89.

Hegelich, M., Karsch, S., Pretzler, G., Habs, D., Witte, K., Guenther, W., Allen, M., Blazevic, A., Fuchs, J., Gauthier, J.C., Geissel, M., Audebert, P., Cowan, T. & Roth, M. (2002). MeV ion jets from short-pulse-laser interaction with thin foils. *Phys. Rev. Lett* **89**, 085002.

Kraft, G. (2001). What we can learn from heavy ion therapy for radioprotection in space. *Physica Medica* **XVII**, Suppl. 1, 13.

Krushelnick, K., Clark, E.L., Zepf, M., Davies, J.R., Beg, F.N., Machacek, A., Santala, M.I.K., Tatarakis, M., Watts, I., Norreys, P.A. & Dangor, A.E. (2000). Energetic proton production from relativistic laser interaction with high intensity plasmas. *Phys. Plasmas* **7**, 2055–2061.

Maksimchuk, A., Gu, S., Flippo, K., Umstadter, D. & Bychenkov, V.Yu. (2000). Forward ion acceleration in thin films driven by a high-intensity laser. *Phys. Rev. Lett* **84**, 4108–4111.

Pukhov, A. (1999). Three-dimensional electromagnetic relativistic particle-in-cell code VLPL (Virtual Laser Plasma Lab). *J. Plasma Phys* **61**, 425–433.

Pukhov, A. (2001). Three-dimentional simulations of ion acceleration from a foil irradiated by a short-pulse laser. *Phys. Rev. Lett* **86**, 3562–3565.

Pukhov, A. & Meyer-ter-Vehn, J. (1996). Relativistic magnetic self-channeling of light in near-critical plasma: Three-dimensional particle-in-cell simulation. *Phys. Rev. Lett.* **79**, 3975–3978.

Pukhov, A. & Meyer-ter-Vehn, J. (1997). Laser hole boring into overdense plasma and relativistic electron currents for fast ignition of ICF targets. *Phys, Rev. Lett* **79**, 2686–2689.

Pukhov, A. & Meyer-ter-Vehn, J. (1998). Relativistic laser-plasma interaction by multi-dimensional particle-in-cell simulations. *Phys. Plasmas* **5**, 1880–1886.

Roth, M., Blazevic, A., Geissel, M., Schlegel, T., Cowan, T.E., Allen, M., Gauthier, J.-C., Audebert, P., Fuchs, J., Meyer-ter-Vehn, J., Hegelich, M., Karsch, S. & Pukhov, A. (2002). Energetic ions generated by laser pulses: A detailed study on target properties. *Phys. Rev. STAB* **5**, 061301.

Roth, M., Cowan, T.E., Key, M.H., Hatchett, S.P., Brown, C., Fountain, W., Johnson, J., Pennington, D.M., Snavely, R.A., Wilks, S.C., Yasuike, K., Ruhl, H., Pegoraro, F., Bulanov, S.V., Campbell, E.M., Perry, M.D. & Powell, H. (2000). Fast ignition by intense laser-accelerated proton beams. *Phys. Rev. Lett* **86**, 436–439.

Santala, M.I.K., Najmudin, Z., Clark, E.L., Tatarakis, M., Krushelnick, K., Dangor, A.E., Malka, V., Faure, J., Allott, R. & Clarke, R.J. (2001). Observation of a hot high-current electron beam from a self-modulated laser Wake-field accelerator. *Phys. Rev. Lett* **86**, 1227–1230.

Sentoku, Y., Liseikina, T.V., Esirkepov, T.Zh., Califano, F., Naumova, N.M., Ueshima, Y., Vshivkov, V.A., Kato, Y., Mima, K., Nishihara, K., Pegoraro, F. & Bulanov, S.V. (2000). High density collimated beams of relativistic ions produced by petawatt laser pulses in plasmas. *Phys. Rev. E* **62**, 7271–7281.

Snavely, R.A., Key, M.H., Hatchett, S.P., Cowan, T.E., Roth, M., Phillips, T.W., Stoyer, M.A., Henry, E.A., Sangster, T.C., Singh, M.S., Wilks, S.C., MacKinnon, A., Offenberger, A., Pennington, D.M., Yasuike, K., Langdon, A.B., Lasinski, B.F., Johnson, J., Perry, M.D. & Campbell, E.M. (2000). Intense high-energy beams from petawatt-laser irradiation of solids. *Phys. Rev. Lett* **85**, 2945–2948.

Wilks, S.C., Kruer, W.L., Tabak, M. & Langdon, A.B. (1992). Absorption of ultra-intense laser pulses. *Phys. Rev. Lett* **69**, 1383–1386.

Wilks, S.C., Langdon, A.B., Cowan, T.E., Roth, M., Singh, M., Hatchett, S., Key, M.H., Pennington, D., MacKinnon, A. & Snavely, R.A. (2001). Energetic proton generation in ultra-intense laser-solid interactions. *Phys. Plasmas* **8**, 542–549.

Zepf, M., Clark, E.L., Beg, F.N., Clarke, R.J., Dangor, A.E., Gopal, A., Krushelnick, K., Norreys, P.A., Tatarakis, M., Wagner, U. & Wei, M.S. (2003). Proton acceleration from high-intensity laser interactions with thin foil targets. *Phys. Rev. Lett* **90**, 064801.

https://doi.org/10.1017/S0263034604222133 Published online by Cambridge University Press